Modelling of Intergranular Corrosion using Cellular Automata -II Numerical Calculation Results and Comparison of Intergranular Corrosion of Stainless Steel using Cellular Automata

Takahiro IGARASHI[1], Eriko IRISAWA[2], Atsushi KOMATSU[3], Masahiro YAMAMOTO[4], Chiaki KATO[5], Fumiyoshi UENO[6]

[1]*Japan Atomic Energy Agency, 2-4 Oaza-shirakata, Tokai-mura, Ibaraki 319-1195, Japan, igarashi.takahiro@jaea.go.jp*
[2]*Japan Atomic Energy Agency, 2-4 Oaza-shirakata, Tokai-mura, Ibaraki 319-1195, Japan, irisawa.eriko@jaea.go.jp*
[3]*Japan Atomic Energy Agency, 2-4 Oaza-shirakata, Tokai-mura, Ibaraki 319-1195, Japan, komatsu.atsushi@jaea.go.jp*
[4]*Japan Atomic Energy Agency, 2-4 Oaza-shirakata, Tokai-mura, Ibaraki 319-1195, Japan, yamamoto.masahiro75@jaea.go.jp*
[5]*Japan Atomic Energy Agency, 2-4 Oaza-shirakata, Tokai-mura, Ibaraki 319-1195, Japan, kato.chiaki16@jaea.go.jp*
[6]*Japan Atomic Energy Agency, 2-4 Oaza-shirakata, Tokai-mura, Ibaraki 319-1195, Japan, ueno.fumiyoshi@jaea.go.jp*

Abstract

Nuclear fuel reprocessing process uses concentrated nitric acid solution at high temperature in order to dissolve spent nuclear fuel, and austenitic stainless steel is used as a main material for equipment of the process. In such a highly oxidizing environment, stainless steel shows the morphology of an intergranular corrosion surface. It is known that grain dropping occurs with intergranular corrosion progress, accelerating the corrosion rate. To keep the safety of the system, it is important to understand the intergranular corrosion behaviour. In this study, intergranular corrosion simulation of stainless steel considering nitric acid solution condition was conducted using two-dimensional cellular automata model and we discussed relation between morphology of corrosion surface, corrosion rate and distribution of grain boundary dissolution rate by comparing experimental data.

Keywords

Stainless Steel; Intergranular Corrosion; Computer Simulation; Cellular Automata

Introduction

Boiling nitric acid solution is applied to dissolve oxide spent nuclear fuel in the component of the plant, such as vessels, tanks, and pipes in nuclear fuel reprocessing process. In the process oxidizing nitric acid solution is used and austenitic stainless steel is in transpassive state. In such kinds of severe condition, austenitic stainless steel shows morphology of intergranular corrosion, and intergranular corrosion occurs by grain dropping and changes in corrosion rate [1]. A lot of studies have been conducted about the causes of intergranular corrosion [2-5]. For example, Armijo studied the effects of alloying additions on the intergranular corrosion of nonsensitive austenitic alloy in boiling nitric acid solution [2]. Hosoi et.al. examined the correlation between grain boundary segregation and intergranular corrosion of Type304l stainless steel in nitric acid solution [3]. In order to keep safety operation of spent fuel reprocessing plants treating oxidizing nitric acid solution, it is important to understand corrosion mechanism.

In this study, we conducted two-dimensional computational simulation of intergranular corrosion of stainless steel considering nitric acid solution condition, and discussed relation between morphology of corrosion surface, corrosion rate and distribution of grain boundary dissolution rate by comparing experimental data.

Simulation Model

In the study, we used two-dimensional intergranular corrosion model using cellular automata method [6]. Cellular automata method is one of the discrete simulation models which consists of a regular grid of cells, and each cell has one of a finite number of states [7]. In the model, two-dimensional simulation space is parted into small cells, and each cells are set to three kinds of states: interior of grain (bulk), grain boundary, and solution. The bulk and grain boundary cell in touch with solution cell transform into solution cell to represent corrosion behaviour in the simulation. Square cell is adopted in the model. Using the discrete cells in the model, we can make various shapes of grains flexibly. In the simulation, grains in simulation system were composed by discrete two-dimensional Voronoi diagram with wave front method [8]. The cells inside of grain were set to bulk cells, and the cells contacted with another grain were set to grain boundary cells. Schematic figure of the model is shown in Fig.1.

Cell dissolution ratio γ is one of the important elements of constructing intergranular corrosion morphology,

$$\gamma = \frac{v_{\mathrm{GB}}}{v_{\mathrm{bulk}}} \tag{1}$$

where v_{GB} and v_{bulk} represent grain boundary dissolution rate and bulk dissolution rate, respectively. Changing bulk or grain boundary cells into solution cells can be determined using corrosion progressing length $r_{\mathrm{bulk/GB}}$, and defined as follows:

$$r_{\mathrm{bulk/GB}} = v_{\mathrm{bulk/GB}} \cdot t = r_{\mathrm{bulk/GB}} \cdot \Delta t \cdot n \tag{2}$$

where t represents simulation time. In the model, t represents discrete time steps $\Delta t \cdot n$ where Δt and n represent time step and number of time step in the simulation, respectively. If $r_{\mathrm{bulk/GB}}$ become larger than cell length, r_{cell},

$$r_{\mathrm{bulk/GB}} > r_{\mathrm{cell}} \tag{3}$$

bulk or GB cell changes into solution cell. In the model, macroscopic transition of corrosion surface can be represented by repeating Eq. (2) and (3) in the simulation.

Intergranular Corrosion Simulation

First, in order to obtain the effect of distribution of v_{GB} to intergranular corrosion behaviour, model simulations were conducted with several kinds of distribution of v_{GB}: normal distribution, log-normal distribution, exponential distribution, and constant v_{GB}. Normal distribution, log-normal distribution, and exponential distribution are represented by Eq. (4)-(6), respectively.

$$f_{\mathrm{norm}}(\mathrm{x}) = \frac{1}{\sqrt{2x\sigma^2}} \exp\left(-\frac{(x-\mu)^2}{2\sigma^2}\right) \tag{4}$$

$$f_{\mathrm{log-norm}}(\mathrm{x}) = \frac{1}{\sqrt{2x\sigma^2}} \exp\left(-\frac{(\ln x-\mu)^2}{2\sigma^2}\right) \tag{5}$$

$$f_{\mathrm{exp}}(\mathrm{x}) = \lambda \exp(-\lambda x) \tag{6}$$

Parameters of functions were set that the averages of each distribution were to almost same value, $|f| \sim 8.0$ in the simulation: $\mu = 8.0$, $\sigma = 2.66$ in $f_{norm}(x)$, $\mu = 2.0$, $\sigma = 0.5$ in $f_{log\text{-}norm}(x)$, $\lambda = 0.125$ in $f_{exp}(x)$. About constant v_{GB}, v_{GB}/v_{bulk} was set to 8.0, same as the average of other distribution. The other parameters were as follows: system size was 1000×1000μm, cell size was 1×1μm, average grain size was 70μm, v_{bulk} was 1.2×10^{-12}m/s, and v_{GB} was set to $v_{bulk} \times f(x)$. Each distribution functions were shown in Fig.2. Corrosion rate by the simulations with each distribution functions were shown in Fig.3. About the results with the conditions of $f_{norm}(x)$, $f_{log\text{-}norm}(x)$, and constant v_{GB}, behaviour of change of corrosion rate with time were almost the same, but the corrosion rate with the conditions of $f_{exp}(x)$ were a little bit smaller than the other. This indicates that, if distribution of v_{GB} is "relatively symmetrical" , corrosion rate is determined by the average of v_{GB}. About the case with $f_{exp}(x)$, distribution of v_{GB} is "non-symmetrical" and this leads corrosion rate smaller. Fig.4 shows histogram of depth of intergranular corrosion by mock-up corrosion test [9]. This relates distribution of v_{GB}. The histogram leads that distribution of v_{GB} may be exponential type with considering "not-count" small value ($\sim v_{GB} < 5.0$μm). Then, we adopted exponential type distribution for v_{GB} and investigated corrosion surface morphology with the difference with condition of width of distribution: $\lambda = 0.125$ as "narrow distribution" and $\lambda = 0.075$ as "wide distribution" shown in Fig.5. Corrosion rate and typical corrosion surface by the simulations with the condition of "narrow distribution" and "wide distribution" are shown in Fig.6 and Fig.7. The model with "wide distribution" condition has faster corrosion rate than that with "narrow distribution" condition. These results lead us to the conclusion that faster corrosion rate was caused by larger average v_{GB} and promoting drain dropping. The corrosion surface with exponential distributed v_{GB} condition had clearly rougher surface than that with constant v_{GB}. The difference of surface roughness between "narrow" and "wide" distributed v_{GB} condition was not clear.

Conclusions

In this study, we conducted two-dimensional computational simulation of intergranular corrosion of stainless steel considering nitric acid solution condition, and discussed relation between morphology of corrosion surface, corrosion rate and distribution of grain boundary dissolution rate by comparing experimental data.

(1) If averages of grain boundary dissolution rate were the same, corrosion rates were almost the same regardless of type of distribution of grain boundary dissolution rate.
(2) The corrosion rate with exponential type “wide” distributed vGB condition had faster value because average value of vGB with “wide” distribution condition became larger than that with “narrow” distribution condition.
(3) The difference of surface roughness between “narrow” and “wide” distributed vGB condition was not clear.

References

1. K. Osozawa and H-J. Engell, Corrs. Sci., 6(8) (1966) 389.
2. J.S. Armijo, Corrosion, 24(1) (1968) 24.
3. K. Hosoi, T. Yokosuka, T. Yoshida, I. Masaoka, and Y. Sasada, Tetsu-to-Hagane, 76(6) (1990) 948 [in Japanese].
4. S. Abe, M. Kaneko, and T. Mizunuma, Tetsu-to-Hagane, 79(6) (1993) 706 [in Japanese].
5. S. Abe, M. Kaneko, H. Komatsu, and F. Kurosawa, Tetsu-to-Hagane, 79(6) (1993) 713 [in Japanese].
6. T. Igarashi, A. Komatsu, T. Motooka, F. Ueno, Y. Kaji, and M. Yamamoto, Zairyo-to-Kankyo, 63(7) (2014) 431 [in Japanese].
7. H. Gutowitz, “Cellular automata : theory and experiment”, 1st ed., MIT Press, (1991).
8. A.I. Adamatzky, Math. Comput. Model., 23(4) (1996) 51.
9. “Final report on survey on corrosion resistant materials equipment maintenance management technology”, Japan Atomic Energy Agency (2006) 2-38 [in Japanese].

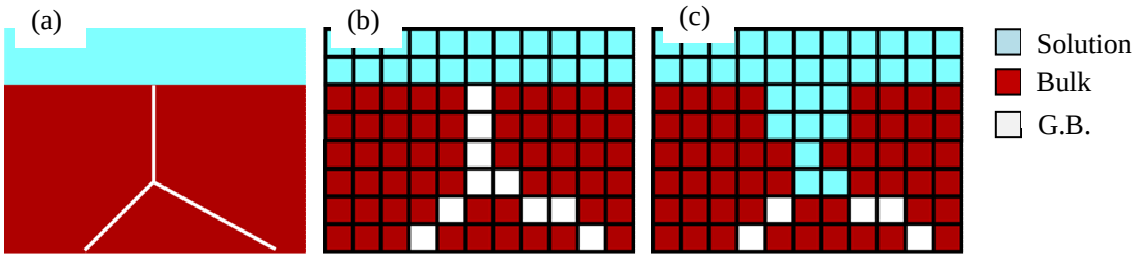

Figure 1: Schematic view of simulation progress. (a)Simulation model with several grains. (b) Cell-parted model with solution, bulk, and grain boundary(G.B.). (c) Corrosion progresses by changing bulk / grain boundary cell into solution cell.

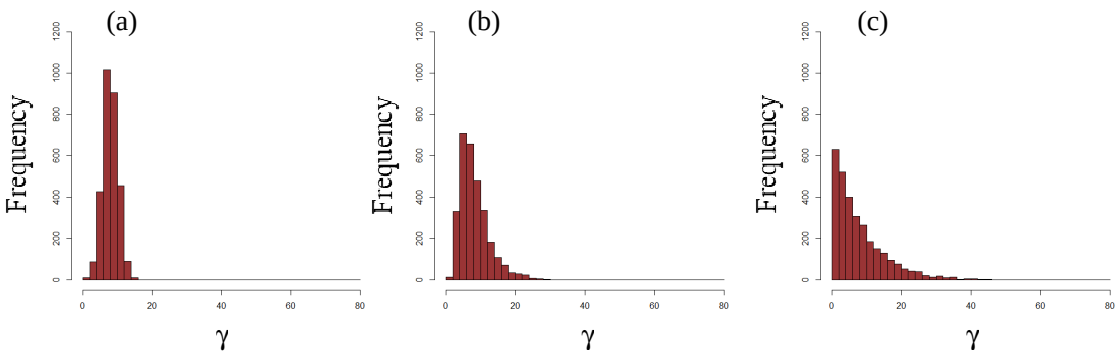

Figure 2: Histograms of several distribution. (a)Normal distribution. (b) Log-normal distribution. (c) Exponential distribution.

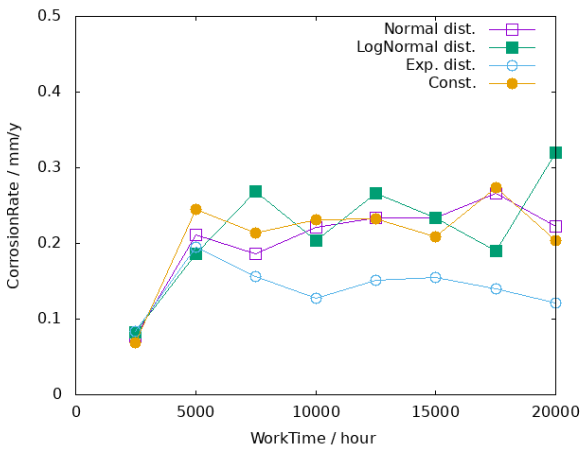

Figure 3: Corrosion rate vs elapsed time.

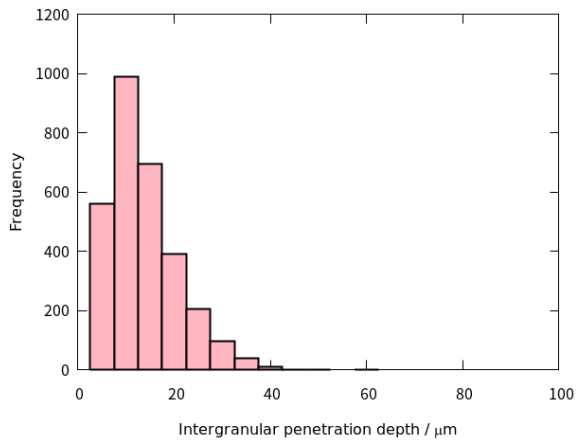

Figure 4: Histogram of intergranular penetration depth by mock-up corrosion test.

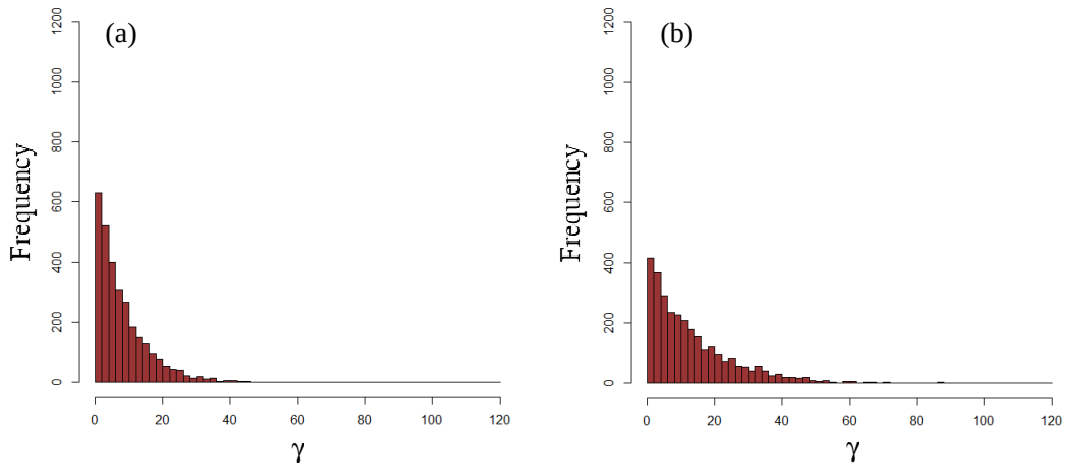

Figure 5: (a) "narrow" distribution (λ=0.125). (b) "wide" distribution (λ=0.075).

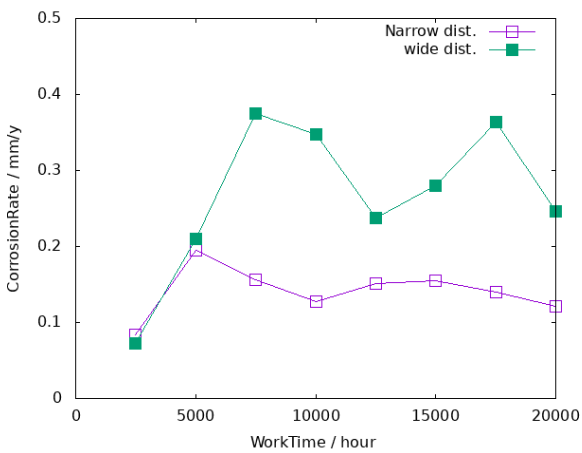

Figure 6: Corrosion rate by the simulation with the conditions of "narrow" and "wide" distribution of v_{GB}.

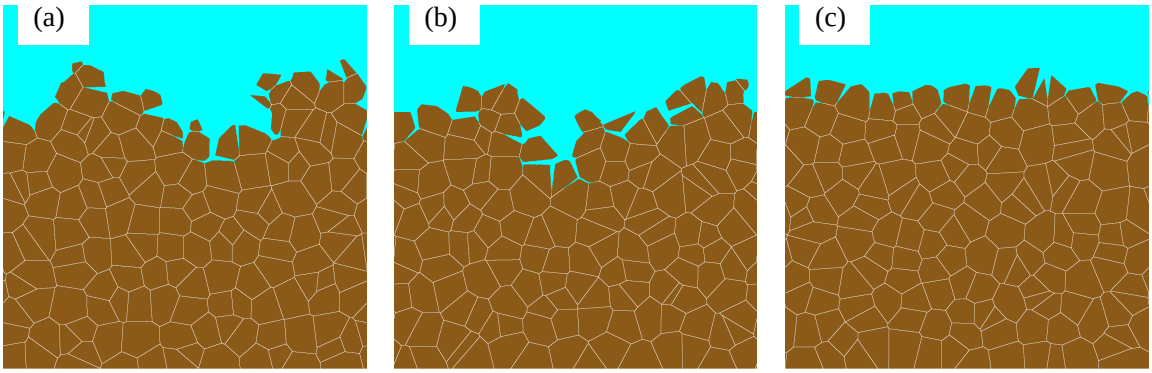

Figure 7: Typical corrosion surface. (a) "narrow" distributed v_{GB}. (b)"wide" distributed v_{GB}. (c) constant v_{GB}.